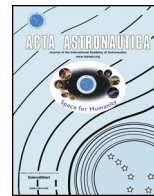




Contents lists available at ScienceDirect

Acta Astronautica

journal homepage: www.elsevier.com/locate/actaastro

A comparative reliability analysis of ballistic deployments on binary asteroids

Onur Çelik^{a,*}, Joan Pau Sánchez^b, Özgür Karatekin^c, Birgit Ritter^c

^a Department of Space and Astronautical Science, The Graduate University for Advanced Studies (SOKENDAI), 252-5210, Sagamihara, Japan

^b Space Research Group, Centre of Autonomous and Cyber-Physical Systems, Cranfield University, MK43 0AL, Bedford, United Kingdom

^c Reference Systems and Planetology, The Royal Observatory of Belgium (ROB), 1180, Brussels, Belgium

ARTICLE INFO

Keywords:

Binary asteroids
Landing
Astrodynamics
Trajectory design
Covariance analysis

ABSTRACT

Small body missions can significantly benefit from deploying small landing systems onto the surface of the visited object. Despite the potential benefit that they may bring, deployments of landers in small body environments may entail significant mission design challenges. This paper thus addresses the potential of ballistic landing opportunities in binary asteroid moons from a mission design perspective, particularly focusing on reliability aspects of the trajectories. Two binaries that were previously identified as target bodies in several missions/proposals, Didymos and 1996 FG3, are considered in this paper. The dynamics near them are modeled by means of the Circular Restricted Three Body Problem (CR3BP), which provides a reasonable representation of a standard binary system. Natural landing trajectories that allow both minimum-velocity local-vertical touchdown and deployment from a safe distance are investigated. Coefficient of restitution values are used as a design parameter to compute the first touchdown speeds that ensure sufficient reliability of landing trajectories. A simple reliability index, which is derived via uncertainty ellipsoid from covariance analysis, is introduced to create a global reliability map across the asteroid surfaces. Assuming 3σ deployment errors on the order of 90 m and 2 cm/s, the results show that ballistic landing operations are likely to be successful for larger binary moons if the deployments target near equatorial regions within longitude range 320° – 20° . It has also been shown that the deployments to smaller binary moons may require higher accuracy in navigation and deployment systems in their mothership, and/or closer deployment distances.

1. Introduction

Near-Earth asteroids (NEAs) are the easiest celestial objects to be reached from Earth (excl. the Moon) and offer a unique window to the early stages of accretion and differentiation of the inner planets of the solar system. Among NEAs, asteroids with moons constitute a considerable portion, of about 16% according to recent estimates [1]. However, no mission has aimed for a binary system, since the visit to the Ida-Dactyl system by Galileo spacecraft. On the other hand, among the variety of missions proposed to asteroids, or to small bodies in general, the interest in binary asteroids also seems to grow. The planetary science community has a profound interest in returning to a binary, particularly with rendezvous missions. Such missions have a strong motivation to settle the debate on the formation of these primitive, information-rich planetary bodies. However, apart from scientific curiosity, and its potential commercial value, missions to binary asteroids are also important as test beds for possible asteroid deflection missions in the future. The threat of asteroid impacts on Earth has been

taken seriously and a variety of techniques have been proposed to deflect potentially hazardous asteroids [2]. One of these is the kinetic impactor technique, which involves a high-speed spacecraft which is to intercept a target asteroid in order to change its orbital course to mitigate the risk of a potential impact [3]. Binary asteroids are ideal testbeds to demonstrate the capabilities of kinetic impactors, as change in orbital period of the natural moon of the asteroid, thereafter called the secondary, after an impact would likely be observed by ground-based observation systems. Along with this line of motivations on science and technology demonstration, several Europe- and US-led, or collaborative missions have been proposed within the last decade, such as Marco Polo-R, Binary Asteroid in-situ Exploration (BASiX), and Asteroid Impact and Deflection Assessment (AIDA) [4, 5, 6].

As being the most recent example, the goal of the joint NASA/ESA multi-spacecraft mission proposal AIDA is to test the kinetic impactor technique in the binary asteroid (65803) 1996GT Didymos [6]. Between the proposed two spacecraft, NASA spacecraft Double Asteroid Redirection Test (DART) is planned to perform a high-speed impact on

* Corresponding author.

E-mail addresses: onur.celik@ac.jaxa.jp (O. Çelik), jp.sanchez@cranfield.ac.uk (J.P. Sánchez), ozgur.karatekin@observatory.be (Ö. Karatekin), birgit.ritter@observatory.be (B. Ritter).

<https://doi.org/10.1016/j.actaastro.2018.03.020>

Received 8 October 2017; Received in revised form 23 January 2018; Accepted 12 March 2018
0094-5765/ © 2018 IAA. Published by Elsevier Ltd. All rights reserved.

the smaller companion of Didymos (informally called Didymoon). Whereas the ESA spacecraft Asteroid Impact Mission (AIM) has science tasks to provide an observational support to theoretical asteroid deflection studies, which ultimately need the mechanical and structural properties, porosity, cohesion of the target, as well as to collect the necessary data to constrain the formation of this particular binary system, and possibly provide an evidence for the formation of other binaries, as well. The original AIM proposal also included MASCOT-2 lander designed by German Aerospace Center (DLR) to perform in-situ observations, and two CubeSats to be deployed near the binary system [7]. As a response to the CubeSat call, the Royal Observatory of Belgium (ROB) proposed two 3U CubeSats to land on Didymoon, named as Asteroid Geophysical Explorer (AGEX) mission [8]. Even if AIM's future appears to be uncertain since 2016 ESA ministerial, the above examples indicate an interest to land small science packages onto the surface of binary systems.

Landing on an asteroid or a comet substantially differs from landing on a deeper gravity well, such as Mars and the Moon. The extremely weak gravitational environment found in small bodies makes purely ballistic descent trajectories a viable option, since the touchdown velocities can be safely managed only by simple structural modifications on the craft. It could also be a preferable solution for motherships, such as AIM, to deploy landers from a safer distance, since the dynamical environment around asteroids imposes non-negligible risks to low-altitude landing operations. This makes ballistic landing trajectories ideal conduits for lander craft that possess only minimal or no control capabilities. However, the very same gravitational environment entails a completely different challenge: Unless sufficient energy is damped at touchdown, the lander may well bounce and subsequently escape from the asteroid, or bounce into a badly illuminated conditions, which would seriously jeopardize the mission [9]. Therefore, research on delivering small, unpowered landers on binary surface has gained a considerable interest.

In binary asteroid systems, one can find natural trajectories to deliver science packages by exploiting the three-body problem. Such strategy was first studied by Tardivel and Scheeres [10], in which they considered the vicinity of equilibrium points of binary systems in Circular Restricted Three-Body Problem (CR3BP) as deployment locations, and defined the first intersection of a trajectory with the surface as landing [10]. This work was followed by a study on the deployment strategy of a small lander in binary asteroid 1996 FG3, back-up target of Marco Polo-R mission proposal [11]. Moreover, within the context of MASCOT-2 lander, Tardivel et al. discussed passive landing opportunities on Didymoon [12]. Tardivel later published an additional study on optimization of ballistic landings in binary asteroid [13]. Along the same line of studies, Ferrari and Lavagna performed a trajectory design study and Monte Carlo simulations against uncertainties for MASCOT-2 [14]. In a more recent study, Çelik and Sánchez proposed a new technique in CR3BP to search opportunities for ballistic soft landing in binary asteroids [15]. This technique defines a landing in local vertical and utilizes a bisection search algorithm to find minimum energy trajectories in backwards propagation from the surface.

This paper focuses on design aspects of ballistic landings of small landers onto the surfaces natural moons of binary asteroids. Çelik and Sánchez (2017) previously showed that landing trajectories onto larger companions of binaries (thereafter called as the primaries) entail higher energy landing trajectories, which; on the one hand may put the payload on the lander at risk due to the higher touchdown velocities, and on the other hand, do not guarantee that the lander will remain in the surface of the primary, unless very low coefficient of restitution can be ensured [15]. Hence, this paper focuses only on landing in the secondary, which was previously shown to potentially enable ballistic soft landing [15]. The paper particularly addresses the reliability aspects of the deployment operations under realistic uncertainties and errors in navigation and deployment systems. Two binaries are selected as targets: Didymos and 1996 FG3. A spherical shape and point mass gravity

are assumed for both companions. A dense grid of first touchdown points is created and distributed homogeneously on the surface, whose locations are described by their latitudes and longitudes. Trajectories are then generated from each point in by applying the methodology developed in [15]. This allows us to obtain nominal trajectories under ideal conditions, as well as to generate a database of reachable regions and characteristics of landings on the surface as a function of landing location. One of the useful information in the database is touchdown speeds, which is the only parameter that characterizes the landing trajectory for a given landing site, due to the definition of the local vertical landing. Thus, they can be used to compute the worst case estimation of the required energy damping, or coefficient of restitution, in order to stay near the binary system after the first touchdown. In this paper, first, the reliability of landing trajectories to reachable locations with the worst case coefficient of restitution are investigated in a simple deployment model with the covariance analysis. The covariance matrices for a global set of landing conditions are propagated to the surface from the deployment points, and the regions with more robust landing conditions are identified.

The reliability of the nominal trajectories are next discussed by generating landing conditions for a specific coefficient of restitution, navigation and deployment errors. A reliability index is introduced from the cross-sectional area of uncertainty ellipsoid (computed after the covariance propagation) in the local topocentric frame of landing site and the cross-sectional area of subject asteroid, in order to assess the robustness of the deployment operation at different landing sites. The covariance analysis and the reliability index are tested by Monte Carlo analyses for further assessment of the methodology. By creating a multifaceted global reliability map of landings, this paper aims to draw a preliminary conclusion about how non-idealities might possibly affect the success of landing operations of an unpowered lander in binary asteroid surfaces.

The remainder of the paper is structured as follows: Section 2 introduces the binary asteroid model; Section 3 introduces the trajectory design methodology and the deployment model, and discusses the results of landing speeds, coefficients of restitution and deployment opportunities for the minimum touchdown speed case. Section 4 describes the navigation model and discusses the results of uncertainty analysis. Finally, Section 5 provides conclusions and final remarks.

2. Binary asteroid model

This paper considers (65803) 1996GT Didymos and (175706) 1996 FG3 as targets for our ballistic landing analysis. These are previously identified targets (with rather frequent launch opportunities) of at least three mission proposals, with a small lander option [4, 5, 6]. Moreover, their physical properties are quite different from each other, as shown in Table 1 below.

As mentioned earlier, this paper assumes binary asteroids which are composed of two spherical bodies with the same constant density. The binary nature of the asteroids allows us to use the CR3BP as the

Table 1

Physical properties of (65803) Didymos & 1996FG3. Didymain and 1996 FG₃ A denote the primaries, whereas Didymoon and 1996 FG₃-B denote the secondaries in the binary systems, respectively.

Property	Didymain	Didymoon	1996 FG ₃ -A	1996 FG ₃ -B
Diameter [km]	0.775	0.163	1.690	0.490
Density [kg/m ³]	2146		1300	
Mass [kg]	5.23×10^{11}	4.89×10^9	3.29×10^{12}	8.01×10^{10}
Mass parameter	0.0092		0.0238	
$\left(\frac{m_2}{m_1 + m_2}\right) [-]$				
Mutual orbit radius [km]	1.18		3.00	
Mutual orbit period [h]	11.9		16.15	

dynamical framework to the motion of a lander, whose details are going to be discussed in the next section. The CR3BP is generally derived in the normalized distance, time and mass units, of which the normalized mass (mass parameter) is provided for both asteroids in Table 1. Mass parameter is one of two main parameters that uniquely defines the dynamical environment near the binary asteroid, together with the ratio between the mutual orbit semi-major axis and the primary diameter (the a -to- D_{pri} ratio). The spherical asteroid and the same density assumptions conveniently allow us to redefine mass parameter in terms of the secondary-to-primary diameter ratio (the D_{sec} -to- D_{pri} ratio). Please, refer to [15] for more comprehensive description and justification of the method. In Çelik and Sánchez [15], the statistics of these two properties among the NEA binaries with known (not assumed) densities were investigated, and it was found that the D_{sec} -to- D_{pri} ratio has a mean of 0.28, while the a -to- D_{pri} ratio has a mean of 2.20 [15]. Those two ratio properties are 0.21 and 1.52 for Didymos, and 0.29 and 1.78 for 1996FG3, respectively, and this locates them near the average ratio properties of the NEA binaries. This suggests that the analyses that will be presented in the next sections not only cover a wider range of binaries in size, but also a good representation of the currently known binary population in terms of the ratio properties. This result has also been illustrated in Fig. 1, which presents the distribution of the ratio properties of the NEA binaries with known densities. It can be noted from the figure that Didymos and 1996FG3 fall near the middle of the data points.

NEA binaries with known densities are represented by a square point in the figure if the referred binary is due to undergo a close encounter with the Earth during an hypothetical launch window between 2020 and 2035. Here, close approach refers to a minimum distance with the Earth of less than 0.2 AU, within which a mission would be justifiable with low energy trajectories [16]. Among the whole set of NEA binaries, 2000 DP107, 1991 VH and 2000 UG11 are also interesting objects, since a patched conic trajectory analysis identifies these objects also as accessible during their close approach.¹ These binaries would also be of interest, since as shown in Fig. 1, their semi-major axis and size ratios are far from the observed average values. Nevertheless, for the sake of simplicity, only two binary asteroids Didymos and 1996FG3 are going to be analyzed in next sections.

3. Landing trajectory design

Let us consider a mothership, in its operational orbit, at a safe distance from the binary system's barycentre. A passive lander (or a "science package") can be sent onto the surface of one or both of binary companions from this mothership by exploiting the natural dynamics around the binary system. As mentioned earlier, landing trajectories in this dynamical scheme can be designed in the framework of the CR3BP, in which the third body (i.e. lander) is assumed to move under the gravitational attraction of the primary and the secondary (i.e. the binary companions) without effecting their motion about their common centre of mass. The dynamical model is traditionally derived in the rotational frame, whose center is at the barycenter of larger bodies, with x -axis on the line connecting the primary and the secondary, z -axis defined in the direction of the mutual orbit normal and y -axis completing triad [17]. Hence, unless otherwise stated, the models and the results will be provided in this rotating barycentric reference frame.

The CR3BP exhibits five equilibria, called the Lagrange points (L1–L5), and five different regimes of motion, expressed in zero-velocity surfaces (ZVS) [17]. For our notional mothership, an operational orbit can be defined in the exterior realm of ZVS, in which the L2 point is closed so that no natural motion is allowed to the interior realm. In this setting, the L2 point presents the lowest energy gate to reach the

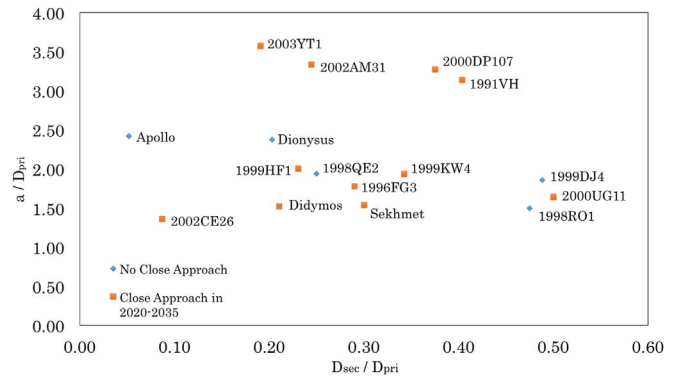


Fig. 1. Close approaches of the NEA binaries (< 0.2 AU) in 2020–2035 time frame. (a : semi-major axis of secondary orbit around primary; D_{pri} is diameter of a spherical primary and D_{sec} is diameter of a spherical secondary).

interior region. Thus, a simple spring mechanism available on a mothership can provide a gentle push to increase the lander's energy in order to open up ZVS at the L2 point and allow motion to the interior realm. The operational orbit of a mothership and deployment strategy are illustrated in Fig. 2.

The landing trajectory design in such scenario is tackled in the groundwork study performed by Çelik and Sánchez in the context of a hypothetical binary asteroid, whose properties are a good representation of the known NEA population [15]. In this study, landing is defined in the local vertical of a landing site and described by its latitude and longitude. Such description has the clear advantage of defining a landing by only one parameter, i.e. touchdown speed ($v_{T/D}$), once a specific landing location is defined. The initial state vectors are then propagated backwards from the landing locations on the surface to the exterior realm of ZVS in a specially developed bisection algorithm [15]. The algorithm searches for the minimum energy landings in a reverse-engineered, iterative manner from the surface to exterior region of ZVS. It then allows trajectories to be designed for any arbitrary latitude–longitude pairs on the surface for any sizes of binary asteroids. Hence, it generates an overall picture for various features of landing, e.g. energies, speeds and required maximum coefficient of restitution (ϵ) values. Moreover, after the resulting trajectories are propagated for a sufficiently long time, any part of the trajectory that lies beyond the ZVS with the L2 point energy can be seen as a potential deployment location. The minimum deployment velocities at those locations can be estimated by computing the necessary velocity that closes ZVS at the L2 point, which therefore corresponds to open up ZVS at the L2 point in forward propagation mode, to allow motion to the interior realm. For much more detailed explanation on the methodology, the reader is encouraged to refer to the work of Çelik and Sánchez [15].

3.1. Landing speed and energy damping

The results of landing speeds are provided in Fig. 3. The secondary is assumed to be tidally locked, hence the attitude of secondary can be assumed fixed in the synodic reference frame. 0° represents the prime meridian whose point is arbitrarily defined as to be on the x -axis, directly facing the L2 point.

Fig. 3 shows that both binaries show similar characteristics in terms of minimum touchdown speeds. Minimum touchdown speeds are observed at the landing sites near the L2 point and in the trailing edge of the far side. Approximately half of the secondary surface is available under 10 cm/s for Didymoon ($\sim 47\%$) and 20 cm/s for 1996 FG3 ($\sim 44\%$). The minimum computed touchdown speeds in Didymoon and 1996 FG3-B are 5.8 cm/s and 14.9 cm/s respectively, at the closest point to the L2 point. It is noteworthy that these values are below the two-body escape speed of both Didymos (32.4 cm/s) and 1996 FG3 (57.6 cm/s). These escape speeds were computed at the landing point

¹ Patched conic accessibility analysis considered Earth departure v_∞ less than 6 km/s and launch performances as expected for Ariane 6.2.

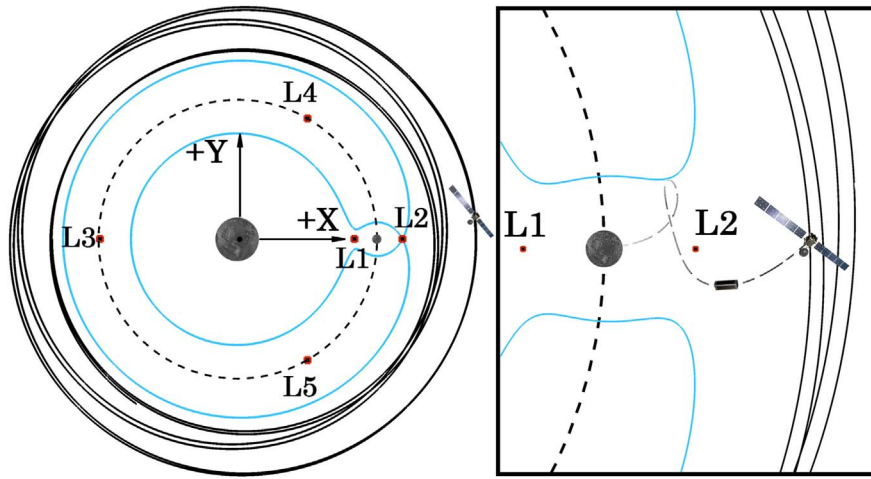


Fig. 2. Mission architecture. Operational scenario of the mothership, ZVS closed at L2 (Left). The deployment provides the energy to open ZVS up at L2 (Right).

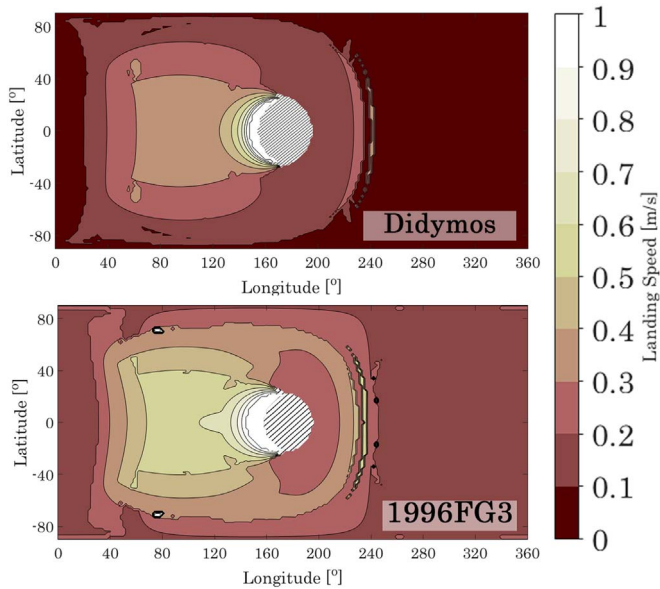


Fig. 3. Minimum touchdown speeds on Didymos and 1996FG3-B surface. The diagonal texture in the middle of figures shows unavailability of ballistic landing to those regions with the trajectory design algorithm discussed in the text. The estimated two-body escape speeds are 32.4 cm/s and 57.6 cm/s for Didymos and 1996FG3, respectively.

closest to the L2 point as the sum of escape speeds of both bodies. However, as shown by the results in Fig. 3, the classical escape velocity is a misleading result, since in order to open up the ZVS at the L2 point, one requires energies that can be achieved with speeds smaller than 5 cm/s. Therefore, a lander can in fact escape with speeds lower than the two-body escape velocity if a proper geometry of the escape motion is found.

As discussed earlier, the trajectory design methodology also enables us to estimate the minimum coefficient of restitution ϵ on the surface. ϵ in this study refers to the simple interaction between surface and the landing spacecraft with a specific value, similar to a bouncing ball on a surface and can be described in both local vertical and local horizontal. However, this paper only concerns with ϵ values in local vertical, and assumes that the outgoing velocity is in the same plane as the incoming velocity and the surface normal vector. In the presence of uncertainties, as it will be analyzed later, the trajectories will no longer touchdown to the surface in local vertical, and local horizontal component of ϵ should also be considered. However, this paper is only concerned with trajectories until touchdown, and do not follow the subsequent bounces, as this would require to model more complex interaction between the

lander and the surface, including friction and rolling. That is out of scope of the present paper and left for the future studies. ϵ value is then defined as in Eq. (1) in its simplest way.

$$\begin{aligned} \mathbf{v}_{LV}^- &= (\hat{\mathbf{n}} \cdot \mathbf{v}) \cdot \mathbf{v} \\ \mathbf{v}_{LV}^+ &= -\epsilon(\hat{\mathbf{n}} \cdot \mathbf{v}) \cdot \mathbf{v} \\ \Rightarrow \mathbf{v}_{LV}^+ &= -\epsilon \mathbf{v}_{LV}^- \end{aligned} \quad (1)$$

where \mathbf{v}_{LV} is the local vertical velocity, $\hat{\mathbf{n}}$ is local normal unit vector and superscripts (-) and (+) denote incoming and outgoing velocities, respectively. ϵ values must typically be between 0 and 1, but it may be considerably different in local horizontal and vertical directions [18, 19].

We can now compute ϵ values to close ZVS at the L1 point for landings depicted in Fig. 3. Basically, this is a rough estimate of how much energy needs to be dissipated at touchdown, so that motion of a lander would be trapped near the secondary of binary system. In the rest of the paper, ϵ will always refer to the required coefficient of restitution to reduce the energy below that of the L1 point. The results are presented in Fig. 4.

In a clear agreement with the results in Fig. 3, the regions of lowest touchdown speeds show higher ϵ values, hinting that very little energy

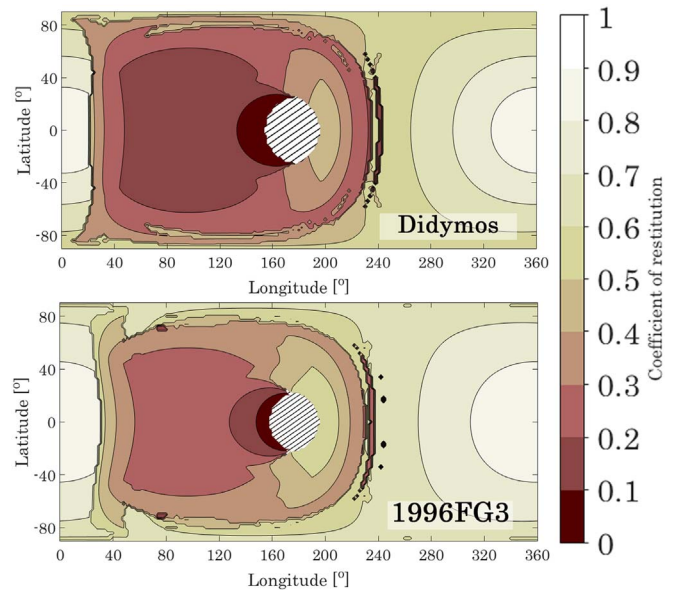


Fig. 4. Required coefficient of restitution (ϵ) to close ZVS at the L1 point for both secondaries.

dissipation would be enough to keep a lander near the binary systems. In the regions of higher touchdown speeds, on the other hand, the ϵ values begin to decrease to levels, for which a lander would likely require an active landing system. Thus, for a purely passive landing, the regions with low landing speed and high ϵ appear to be more attractive options to consider for deployment.

Fig. 4 reveals important insights at first glance into the feasibility of the ballistic landing in binary asteroid systems. It should be noted at this point that the coefficient of restitution value in the sampling horn of Hayabusa at the touchdown was measured as ~ 0.85 [20]. While this value has large uncertainties, Philae’s touchdown on comet 67P/Churyumov-Gerasimenko revealed that the comet surface is “strongly damping” with ϵ values varying between ~ 0.2 – 0.5 [21]. Taking this information into account, it is clear that assuming a conservative estimate of ~ 0.9 for ϵ would allow only some reduced regions in the far side of the secondary. However, more recent theoretical and experimental studies suggest that appropriate structural design solutions may well allow $\epsilon \sim 0.6$, or even lower, in the asteroid surfaces [22, 23].

The maximum expected ϵ value on the current mission scenarios is therefore ~ 0.6 . The results on Fig. 4 allow enough room to be more conservative to provide a margin to this value, therefore $\epsilon = 0.7$ was chosen as the minimum feasibility criteria of landing operations. Regions that exhibit lower than this ϵ value are going to be discarded as infeasible. Nevertheless, as shown in Çelik and Sánchez [15], the results in Fig. 4 are likely to be the worst case estimates of the actual ϵ values, since the motion after a bounce may allow further contact with the surface, i.e. more opportunities for energy damping, before the lander rests on the surface. For more information, the reader may refer to the other available works in the literature [18, 24, 25, 19, 21].

3.2. Deployment model

In the deployment operation, the mothership is likely to release the lander while on a trajectory taking it near to a binary, but still safe according to the ZVS discussion in Section 3. Thus, we assume that a release trajectory has a periapsis at the deployment point, and an apoapsis near the sphere of influence (SOI) of binary system. Then, at the deployment point the mothership shall have a normalized velocity $\mathbf{v}_{S/C}$, computed through elliptic Keplerian orbits as:

$$\mathbf{v}_{S/C} = \left(\sqrt{\frac{2}{r_{release}} - \frac{2}{r_{release} + r_{SOI}}} - r_{release} \right) \hat{\theta} \quad (2)$$

where $\hat{\theta} = \hat{\mathbf{h}} \times \hat{\mathbf{r}}$, $\hat{\mathbf{r}}$ is the release position unit radius vector and $\hat{\mathbf{h}}$ is the direction of the ballistic descent trajectory momentum vector. The initial state vector of the ballistic descent $[\mathbf{r}_{release} \ \mathbf{v}_{release}]$ was computed with the aforementioned bisection algorithm [15]. The state vector $[\mathbf{r}_{release} \ \mathbf{v}_{release}]$ is chosen such that two constraints are satisfied:

- Duration of the descent trajectory must be less than 12 h.
- Mothership distance to the barycenter of the binary must be greater than 1.25 times the distance of the L2 point to the barycentre, r_{L2} .

The duration of the descent is set to ensure relatively shorter operation times, while also allowing plenty of opportunities for deployment. And the minimum deployment altitude is scaled with the L2 point distance so that the mothership will always be in a safe distance from the secondary. This distance can be increased or decreased during the design phase in a trade-off between the risk on the mothership and the robustness of the deployment operations. However, note that the deployment distance must always be greater than or equal to the L2 point distance to barycentre due to the particular characteristic of the ballistic landing discussed here. Here, it was chosen arbitrarily with the purpose to define a safer deployment scenario than those studied in previous work by the authors [26], since the further from the secondary surface the more dynamically stable. The deployment altitude in this

case corresponds to ~ 440 m for Didymos, ~ 1285 m for 1996 FG3 on the secondary surface when measured on the x-axis of the rotating reference frame.

The above deployment model and the constraints are an attempt to generalize the deployment model for any binary system of interest. Depending on the dynamical characteristics of a target, multitudes of orbits can be exploited to fulfill operational and scientific requirements. Examples of those include direct and retrograde interior orbits around primaries, quasi-satellite orbits around the secondary, and direct and retrograde exterior and terminator orbits around the binary system, or even orbits around equilateral Lagrange points of the binary systems [27, 28]. Some of the example orbits may enable better deployment conditions for certain regions (e.g. poles), but this is out of scope of the paper.

The deployment spring mechanism in the mothership must then provide an impulse to the lander such that:

$$\mathbf{v}_{spring} = \mathbf{v}_{release} - \mathbf{v}_{S/C} \quad (3)$$

Note that, ignoring navigation errors, the release location $\mathbf{r}_{release}$ is assumed to coincide with the position of the mothership, $\mathbf{r}_{S/C}$, at the release time. According to the above deployment model, a relatively reduced region of the secondary is available for landing at coefficient of restitution $\epsilon > 0.7$, and those regions are depicted in Fig. 5. Some regions in the far side are no longer reachable, due to the fact that the ballistic descent trajectory takes more than 12 h from the given deployment distance. This however could be solved by allowing touchdown speeds larger than the minimum touchdown velocity (in Fig. 3), as will be seen in the next section.

Most of the available deployments are possible with deployment speeds on the order of ~ 5 cm/s or below, and no deployments are observed with speeds higher than 10 cm/s. While the most deployments to the Didymos surface are possible with ~ 2 cm/s, the deployments to the 1996 FG3-B surface are possible ~ 3 cm/s and above. Note that the Philae’s separation speed from Rosetta was designed to be between 5 and 50 cm/s with a redundant system capable of 18 cm/s [19]. AIM’s deployment mechanism, on the other hand, is designed to provide 2–5 cm/s within ± 1 cm/s accuracy [29]. Thus, it seems that a separation mechanism whose performance in between that of AIM and Rosetta can easily fulfill the deployment demands of both targets.

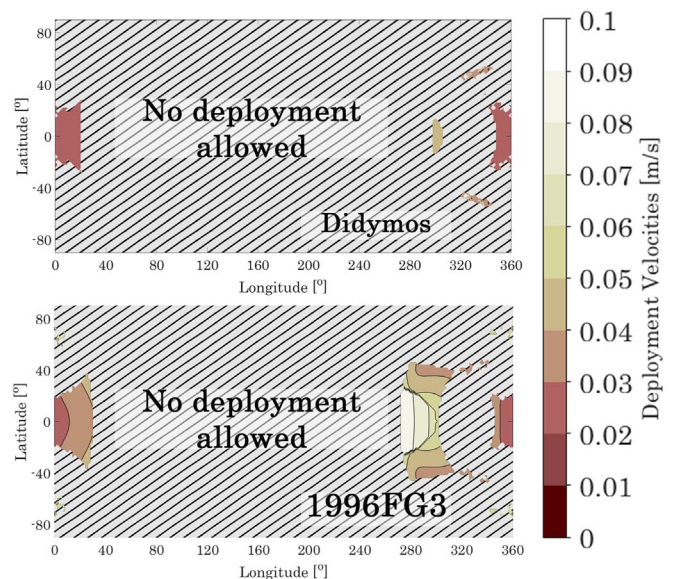


Fig. 5. Deployment opportunities with minimum possible touchdown speeds.

4. Reliability of ballistic landing trajectories

Ballistic landing trajectories show a compelling prospect to be utilized as a landing strategy, however they also come with their inherent instabilities [30]. Furthermore, trajectories that are generated by the strategy described above are largely idealized with relatively ad-hoc constraints, and it is thus necessary to assess their robustness also against the non-ideal conditions. Particularly, deployments will be affected by the orbit determination errors of the mothership, as well as by the inaccuracies in the deployment mechanism.

Many other error sources and perturbations also exist, such as attitude errors or perturbations due to the highly irregular nature of asteroids, particularly in terms of gravity field and shape. This study, however, is only concerned with the GNC and the deployment aspects of non-idealities. The authors' previous works also considered the density (hence the gravity) errors in the secondaries [26, 31], however Didymoon and 1996 FG3-B constitute only $\sim 1.2\%$ and $\sim 2.5\%$ of the total mass of their respective systems according to the information in Table 1. It was shown to have a limited effect in the overall robustness of trajectories to reach the surface as compared to the GNC and deployment errors [31, 26], therefore these were not considered in the current study. However, errors in the gravity field of the secondaries may be critical especially in long duration ballistic landing trajectories, and a special care should be taken [32]. Furthermore, solar radiation pressure is found to have a negligible impact due to short time scale of landings. As a final remark, the fact that the spherical shape is assumed may not necessarily be considered as a source of error, because if the shape of the binary was known, the same strategy could be used to compute new trajectories, as was done for Philae's descent trajectory computation [33]. Table 2 summarizes the error and uncertainty values considered in the paper.

The values in the table are realistic and found during the design process of AIM. It should be noted that the GNC position error in Table 2 is three times or more than those considered in the previous studies by the authors [31, 26, 34]. This is due to the GNC system design of AIM, which assumes no altimeter, but pure relative navigation, with a fusion of image tracking and the other sensors onboard [35]. The GNC system therefore requires a comparison of two (or more) consecutive images and measurement of indirect sources (star tracker and inertial measurement units (IMUs)) to measure the range to the body, hence inherently increasing the error magnitude.

4.1. Deployment covariance analysis

A convenient way to analyze impact of the uncertainty and error sources is covariance analysis. The covariance matrix in this context provides a linear approximation of the sensitivity of a nominal landing trajectory against the non-idealities. We can translate the information in Table 2 into a diagonal covariance matrix at release time (t_R) Q_R as:

$$Q_R = \begin{bmatrix} \sigma_x^2 & 0 & 0 & 0 & 0 & 0 \\ 0 & \sigma_y^2 & 0 & 0 & 0 & 0 \\ 0 & 0 & \sigma_y^2 & 0 & 0 & 0 \\ \hline 0 & 0 & 0 & \sigma_{v_x}^2 & 0 & 0 \\ 0 & 0 & 0 & 0 & \sigma_{v_y}^2 & 0 \\ 0 & 0 & 0 & 0 & 0 & \sigma_{v_z}^2 \end{bmatrix} \quad (4)$$

Table 2
Uncertainty and error sources.

Source	3σ
GNC position accuracy	± 90 m
GNC velocity accuracy	± 2 cm/s
Spring magnitude error	3%
Spring angle error	$\pm 4^\circ$

where the diagonal values contain variance of errors in each component of the state vector. At the instant of deployment, lander and mothership are assumed to be at the same position, hence the GNC errors applies to the lander initial state.

The spring angle and magnitude errors, as well as the GNC errors in velocity, will affect the velocity components of the Cartesian covariance matrix in Eq. (4). For the spring errors, a Monte Carlo sampling with 10000 random values was used to estimate the variance of the velocity components due to the spring errors. These variances are then sum to those of the GNC.

Q_R can then be propagated to the asteroid surface via state transition matrix Φ of the nominal trajectory. At the time of touchdown, $t_{T/D}$, the covariance matrix can be computed as below:

$$Q_{T/D}(t_{T/D}) = \Phi(t_{T/D}, t_R) Q_R(t_R) \Phi^T(t_{T/D}, t_R) \quad (5)$$

where subscripts T/D and R denote touchdown and release respectively. The position errors at touchdown are represented by the 3×3 submatrix in the top left corner of the covariance matrix at touchdown time $Q(t_{T/D})$:

$$Q_{T/D} = \begin{bmatrix} Q_{xx}^{T/D} & Q_{xy}^{T/D} & Q_{xz}^{T/D} & & & \\ Q_{yx}^{T/D} & Q_{yy}^{T/D} & Q_{yz}^{T/D} & & & \\ Q_{zx}^{T/D} & Q_{zy}^{T/D} & Q_{zz}^{T/D} & & & \\ \hline & & & Q_{BL} & & \\ & & & & & Q_{BR} \end{bmatrix} \quad (6)$$

However, the position would best be represented in the topocentric coordinate frame using the principal axes of the secondary of the binary of interest. Therefore, the resulting matrix $Q_{T/D}$ after propagation is rotated to the local topocentric frame of the landing site [36]. The 3×3 top left submatrix in Eq. (6) is decomposed into its eigenvalues and eigenvectors. In such approach, the submatrix in Eq. (6) can be represented in the following form:

$$Q_P(t_{T/D}) = \begin{bmatrix} a^2 & 0 & 0 \\ 0 & b^2 & 0 \\ 0 & 0 & c^2 \end{bmatrix} \quad (7)$$

where the subscript P denotes position. Square root of the diagonal non-zero elements a^2 and b^2 in Eq. (7) are semi-major and semi-minor axes (a , b) of the footprint of the uncertainty ellipsoid representing the 1σ Gaussian distribution of the deployment errors as projected onto the landing site. Given the assumed Gaussian distributions for uncertainties and errors, the probability to obtain a landing trajectory touching down outside the 1-sigma distribution footprint is high (i.e. $\sim 61\%$ in a 2D distribution). The probability to fall instead outside the 2-sigma footprint ($2a$, $2b$) is of about of 14%, while outside the 3-sigma footprint ($3a$, $3b$) would only be of about 1% [36]. Since a small lander may well be used in a much more daring operation than a traditional spacecraft, we will assume for now that a landing opportunity with a 2σ footprint smaller than the cross-sectional area of the secondary would be a landing opportunity with an acceptable risk.

Thus, a reliability index can be defined such as:

$$A_{2\sigma} = \frac{\pi(2a \cdot 2b)}{\pi \cdot r_s^2} = \frac{4ab}{r_s^2} \quad (8)$$

where $A_{2\sigma}$ represents the area of the 2-sigma distribution footprint in units of the cross-sectional area of the secondary and r_s is the radius of the spherical secondary. Thus, a 2σ distribution footprint $A_{2\sigma} > 1$ would represent a footprint larger than the asteroid itself, indicating a highly unreliable deployment. One would ideally aim for deployments such that $A_{2\sigma} < 1$. Note that as long as there are uncertainties in deployment (which is the case here), $A_{2\sigma}$ will always be greater than 0, and $A_{2\sigma} \in [0, \infty)$.

The expression in Eq. (8) allows defining a single figure of merit to measure landing reliability, which, as is shown later by a Monte Carlo

analysis validation, provides a simple and fast method to obtain a qualitative understanding of the reliability of the landing opportunity.

In the next two subsections, we will analyze how the $A_{2\sigma}$ -index value appears in both asteroids for minimum and modified touchdown velocities.

4.2. Landing at minimum and modified touchdown speeds

Fig. 4 summarizes the results of the 2σ distribution footprint, $A_{2\sigma}$, analysis for two binaries in the minimum touchdown speed case. The fact that only small regions display values $A_{2\sigma} \leq 1$ indicates that at the achieved accuracies in navigation and deployment in Table 2, landing trajectories are not robust enough to provide wider range of reliable landing locations.

With the introduced deployment model and the chosen arbitrary safe distance for deployment, Didymoon surface is almost unreachable at any point except for very small, scattered islands in the far side. Even among those reachable regions, only an area in near-equatorial latitudes, at longitude 300°, there is a very limited area that exhibit the $A_{2\sigma}$ -index between 1 and 2. This region is rather more reliable, because trajectories are more energetic with higher touchdown speeds, therefore allow less propagation time for uncertainties. The results for Didymoon suggest that, a deployment aiming minimum touchdown speeds may entail challenges, at least for given deployment model, distance and navigation uncertainties, that may be hard to overcome.

The deployments aiming minimum touchdown speeds to 1996 FG3-B surface appears to be more robust, although again in a reduced region. The most reliable region appears to be around the same region as observed in Didymoon. However, unlike the Didymoon case, this region extends about 20° in both latitudinal and longitudinal directions. This robust region was previously identified for the hypothetical asteroid in Çelik and Sánchez [15], whose size is closer to 1996 FG3 (though slightly smaller) [15]. The existence of the same region in both binaries implies a first hand estimation about the reliable landing operations regardless of the target properties, even before generating a global map.

Investigating the minimum touchdown speeds allows us to understand the limits of this particular mission design problem. This information is undoubtedly valuable during a mission design process; however, the minimum touchdown speeds do not always imply the optimal landing operations, as demonstrated in Fig. 6. It follows then that larger touchdown speeds than the minimum shall be attempted. A larger than the minimum touchdown speed implies a much faster

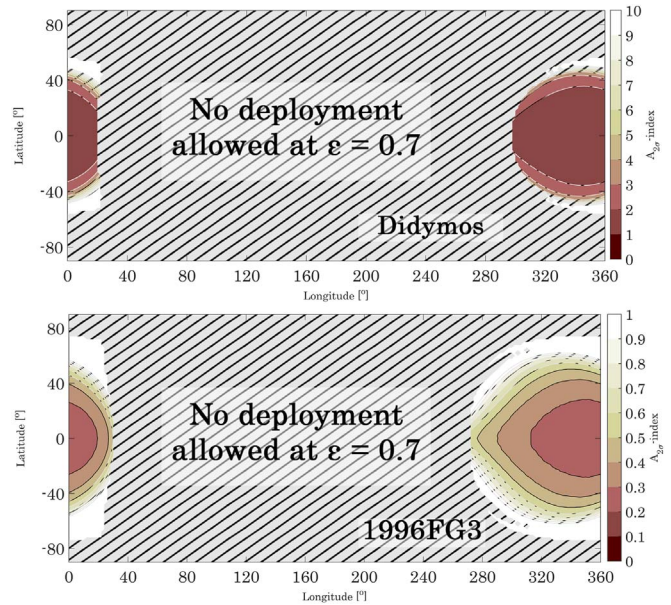


Fig. 7. $A_{2\sigma}$ -index for modified touchdown speeds.

descent trajectory, thus shorter landing operations. With a straightforward reasoning, initial errors at the instant of deployment may have lesser time to propagate, hence have a smaller impact on the dispersion. Nevertheless, the spring error is proportional to the velocity magnitude, and thus the latter statement requires to be demonstrated.

As discussed in Section 3.1, $\epsilon = 0.7$ is defined as the maximum allowed value. Hence, a landing operation that precisely match this value is computed. That means to scale landing speeds, so that the energy damping at the instant of touchdown will ensure precisely the velocity magnitude that closes the ZVS at the L1 point and restrict the motion around the secondary body. The maximum allowed touchdown speeds can therefore be as in Eq. (9) for each landing point:

$$v_{T/D}^{site} = \frac{v_{L1}^{site}}{\epsilon} \quad (9)$$

where $v_{T/D}^{site}$ is touchdown speed and v_{L1}^{site} is the speed that closes the ZVS at the L1 point at a given landing site. $v_{T/D}^{site}$ is considered as the nominal touchdown speed for this case, and since ϵ value is conservatively defined well within the current knowledge and the worst-case estimates as shown in Fig. 4, no margin has been assumed. Fig. 7 now shows the robustness of those trajectories computed for the landing speeds as computed in Eq. (9), to the same errors in deployments as described in Table 2.

Note that the color code is now different, and separated as the $A_{2\sigma}$ -index values changed. The figure demonstrates a dramatic increase in the reliability of deployments to both targets. Total area of possible landing sites have clearly expanded in both asteroids, about ~30% of all 1996 FG3-B surface and ~17% of all Didymoon surface is now available for deployments with the introduced deployment model.

Despite the increased possibilities for deployments on Didymoon surface, no target site with $A_{2\sigma} < 1$ is observed. The lowest value in this case is 1.29, and it is observed in equator at 334° longitude. The $A_{2\sigma}$ -index values remain in between 1 and 2 times the cross sectional area of Didymoon for a wide region, extending longitudes from 300° to 20° and latitudes up to 35°. This regions would provide the highest reliability, though still with lower than what would be expected from a reliable deployment ($A_{2\sigma} \ll 1$). This result suggests that the introduced deployment model, especially the deployment distance may be responsible for this poor reliability in the Didymos case. Deployments at lower altitude will likely to improve the reliability of landing. Finally, as target latitude increases, reliability of deployments decreases. Mid-

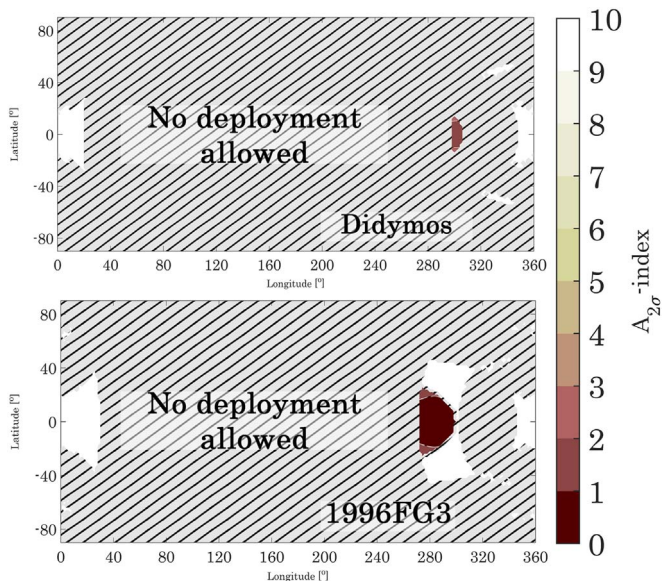


Fig. 6. $A_{2\sigma}$ -index for minimum touchdown speeds.

latitudes display the lowest reliability with $A_{2\sigma}$ -index ≥ 10 .

Deployments on the 1996 FG3-B surface, on the other hand, provides much more reliable prospects with a much larger area of landing opportunities. All possible regions have now shown $A_{2\sigma} < 1$, except small regions in high-latitudes. The lowest $A_{2\sigma}$ value is computed for 1° latitude and 0° longitude (i.e. approximately the tip of 1996FG3-B on the far side) as 0.24. $A_{2\sigma}$ -index values smaller than 0.6 extend between 280° in the trailing edge to 20° in the leading edge, providing numerous reliable deployment opportunities. Unlike for the Didymos case, there are still reliable opportunities at mid-latitudes, up to approximately 45° – 50° . This opens up possibly interesting regions to be explored by a small lander, for the sizes of asteroid moons as 1996 FG3-B.

The $A_{2\sigma}$ -index offers quick assessment capability for a target landing site with a very simple parameter. However, it is reasonable to verify how our covariance based fast reliability analysis matches with Monte Carlo analyses, which can account nonlinearities intrinsic to the dynamical model. Therefore, Monte Carlo analysis was performed for each target landing locations in order to verify the assertions made here about the reliability of deployments with the $A_{2\sigma}$ -index. The Monte Carlo analysis in this case constitutes 1000 randomly generated samples with the uncertainty values provided in Table 2. It is important note that, a Monte Carlo analysis with 1000 samples represent statistics with $\sim 5\%$ error 3σ variance [37]. As a side note, while the $A_{2\sigma}$ -index computation took ~ 6 h in total for this case, the Monte Carlo computations for this case took ~ 3 days for the same case for one hemisphere of one asteroid. The results are presented in Fig. 8.

In general, there is a very good agreement with our Monte Carlo analysis and $A_{2\sigma}$ -index results. Almost all regions in the 1996 FG3-B surface with $A_{2\sigma}$ -index lower than 1 show Monte Carlo success rate greater than 95%. The Monte Carlo analysis of the target site with the highest $A_{2\sigma}$ -index certifies that the probability of first touchdown is 100%. In fact, it appears that very high $A_{2\sigma}$ values can be evaluated as reliable for the 1996 FG3-B surface, since the $A_{2\sigma}$ -index of up to 0.8 in the 1996FG3 case exhibits Monte Carlo success of greater than 90%. If we then assume a coefficient of restitution of 0.7 or lower, one can be confident that the lander will remain in the surface of 1996 FG3-B, or binary systems whose properties similar to that.

The situation, on the other hand, is much more complex in Didymos surface. While the $A_{2\sigma}$ -index is distributed homogeneously in a relatively larger area in Fig. 7, Monte Carlo results for the same region reveal a fragile condition. Indeed, our assertions for Didymos was confirmed, and the deployments to Didymos surface is not at all

reliable against the initial errors with the assumption made. It appears that the $A_{2\sigma}$ -index is less accurate for a smaller binary according to the Monte Carlo results, but always in agreement with it qualitatively. In this respect, the $A_{2\sigma}$ -index works well. The results, on the other hand, suggest that, when the uncertainties are the same, the deployment distance must be closer to the Didymos surface for more reliable operations.

Finally, although it is not explored in this work, it should also be noted about the Monte Carlo analysis that allowing longer propagation time (>12 h) and higher number of samples in simulations may slightly alter the presented success probabilities of the first touchdowns on both targets.

5. Conclusions

This paper investigated the reliability of ballistic landings on the secondaries of two previously proposed target binaries, Didymos and 1996 FG3. Building a model on top of the previously developed algorithm [15], various simulations were performed in order to assess statistical success of nominal trajectories under the effect of deployment and navigation errors. It was found that, landing trajectories to the regions with lowest possible touchdown speeds are unavailable for short duration of deployment operations, therefore prone to suffer from uncertainties. A simple scale-up procedure is applied to touchdown speeds in order to increase their energy by means of assuming a new, conservative coefficient of restitution, whose value is in harmony with observational findings and theoretical studies. Allowing higher touchdown speeds have greatly increased the reachable area and reliability of deployment operations for given deployment model.

A covariance analysis was performed with realistically defined uncertainties in order to assess the robustness of the available trajectories. Reliable regions are identified via a simple index defined by the projected area of the uncertainty ellipsoid in the topocentric frame of the target landing sides, and cross-sectional area of the target asteroid. This simple index is a useful measure, despite its simplicity, and allows a quick qualitative investigation of robust landing operations. The usefulness of the index is in fact certified by the Monte Carlo analysis. Thus, the robust design optimization of such mission can easily include this covariance based reliability index, which can provide sufficiently accurate reliability results to be used in the process.

The deployment reliability within the available regions are much higher in the far side of the binary moons, with very small deployment speeds. Near-equatorial regions are by far the most robust, with more longitudes in the trailing side. Larger binary moons, at least sizes on the order of 1996FG3 or more, also provide opportunities to explore higher latitude regions, which might be of interest to understand the binary formation. The deployment operations for mid- and high-latitudes, however, seem to be much less reliable in small binaries with the proposed deployment strategy. Particularly, there are no deployment opportunities identified for polar latitudes in both sample asteroids. However, the reliability analysis in this paper suggests that, in order to achieve higher impact probabilities in smaller asteroid cases, a more accurate deployment mechanism and navigation system in mother-ships, and closer deployments are paramount. It should be noted for the latter, that dynamical stability of mothership motion and operational risk due to the proximity to the surface must carefully be assessed.

The analyses in this paper revealed regions of reliable ballistic landing through the covariance-based reliability index. This index would provide a simple, straightforward and efficient analysis framework and the results of that can also be used in the robust optimization of the deployment and descent operations where the reliability of the landing trajectory is also maximized in the design process. The final results on the target binary asteroids would also provide useful inputs to the current and the future small body exploration missions that carry small landers to be deployed to the surface via ballistic trajectories.

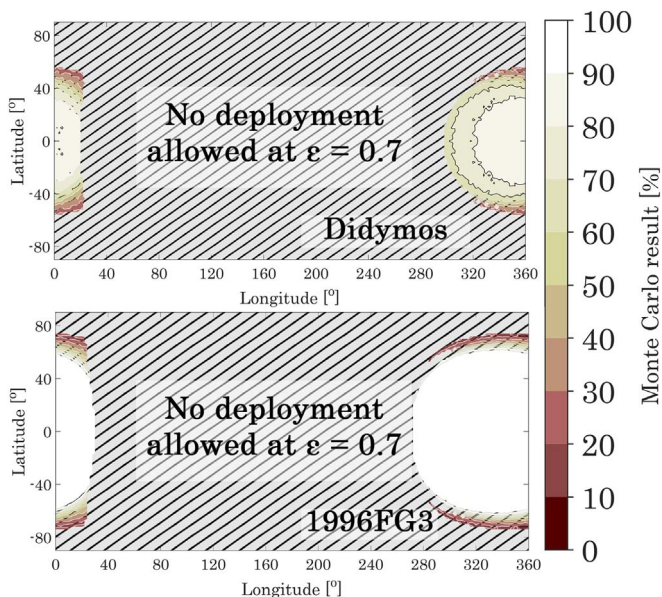


Fig. 8. The Monte Carlo results.

Acknowledgement

Onur Çelik acknowledges the MEXT research scholarship from the Japanese government and the short-term research grant from ROB. The authors would like to thank Massimo Casasco for his valuable inputs about the navigation and deployment errors.

Appendix A. Supplementary data

Supplementary data related to this article can be found at <http://dx.doi.org/10.1016/j.actaastro.2018.03.020>.

References

- [1] J.L. Margot, M.C. Nolan, L.A.M. Benner, S.J. Ostro, R.F. Jurgens, J.D. Giorgini, D.B. Campbell, Binary asteroids in the near-Earth object population, *Science* 296 (5572) (2002) 1445–1448, <http://dx.doi.org/10.1126/science.1072094>.
- [2] A.W. Harris, M.A. Barucci, J.L. Cano, A. Fitzsimmons, M. Fulchignoni, S.F. Green, D. Hestroffer, V. Lappas, W. Lork, P. Michel, D. Morrison, D. Payson, F. Schäfer, The European Union funded NEOSShield project: a global approach to near-Earth object impact threat mitigation, *Acta Astronaut.* 90 (1) (2013) 80–84, <http://dx.doi.org/10.1016/j.actaastro.2012.08.026>.
- [3] J.P. Sanchez, C. Colombo, Impact hazard protection efficiency by a small kinetic impactor, *J. Spacecraft Rockets* 50 (2) (2013) 380–393, <http://dx.doi.org/10.2514/1.A32304>.
- [4] M.A. Barucci, A.F. Cheng, P. Michel, L.A.M. Benner, R.P. Binzel, P.A. Bland, M. Zolensky, MarcoPolo-R near earth asteroid sample return mission, *Exp. Astron.* 33 (23) (2012) 645–684, <http://dx.doi.org/10.1007/s10686-011-9231-8>.
- [5] R.C. Anderson, D. Scheeres, S. Chesley, the BASiX Science Team, A mission concept to explore a binary near earth asteroid system, *Proceedings of the 45th Lunar and Planetary Science Conference, The Woodlands, Texas, 2014 March 17–21, Paper number 1777*.
- [6] A.F. Cheng, J. Atchison, B. Kantsiper, A.S. Rivkin, A. Stickle, C. Reed, S. Ulamec, Asteroid impact and deflection assessment mission, *Acta Astronaut.* 115 (October–November) (2015) 262–269, <http://dx.doi.org/10.1016/j.actaastro.2015.05.021>.
- [7] A.G.I. Carnelli, R. Walker, Science by cubes: opportunities to increase AIM science return, *Proceedings of the 4th Interplanetary CubeSat Workshop, London, UK, 2015 May 27–28, Paper number 2015. B.3.1*.
- [8] O. Karatekin, D. Mimoun, N. Murdoch, B. Ritter, N. Gerbal, The asteroid geophysical Explorer (AGEX) to explore didymos, *Proceedings of the 5th Interplanetary CubeSat Workshop, Oxford, UK, 2016 May 28–29, Paper number 2016. A.2.1*.
- [9] S. Ulamec, L. O'Rourke, J. Biele, B. Grieger, R. Andres, S. Lodi, P. Munoz, A. Charpentier, S. Mottola, J. Knollenberg, M. Knapmeyer, E. Kühr, F. Scholten, K. Geurts, M. Maibaum, C. Fantinatti, O. Kuchemann, V. Lommatsch, C. Delmas, E. Jurado, R. Garmier, T. Martin, Rosetta Lander - Philae: Operations on comet 67P/Churyumov-Gerasimenko, analysis of wake-up activities and final state, *Acta Astronaut.* 137 (August) (2017) 38–43, <http://dx.doi.org/10.1016/j.actaastro.2017.04.005>.
- [10] S. Tardivel, D.J. Scheeres, Ballistic deployment of science packages on binary asteroids, *J. Guid. Contr. Dynam.* 36 (3) (2013) 700–709, <http://dx.doi.org/10.2514/1.59106>.
- [11] S. Tardivel, P. Michel, D.J. Scheeres, Deployment of a lander on the binary asteroid (175706) 1996 FG₃, potential target of the European MarcoPolo-R sample return mission, *Acta Astronaut.* 89 (August–September) (2013) 60–70, <http://dx.doi.org/10.1016/j.actaastro.2013.03.007>.
- [12] S. Tardivel, C. Lange, S. Ulamec, J. Biele, The deployment of MASCOT-2 to Didymos, *Proceedings of the 26th AAS/AIAA Space Flight Mechanics Meeting, Napa, California, 2016 February 14–18, Paper number: AAS 16–219*.
- [13] S. Tardivel, Optimization of the ballistic deployment to the secondary of a binary asteroid, *J. Guid. Contr. Dynam.* 39 (12) (2016) 2790–2798, <http://dx.doi.org/10.2514/1.G000593>.
- [14] F. Ferrari, M. Lavagna, Consolidated phase a design of Asteroid Impact Mission: MASCOT-2 landing on binary asteroid didymos, *Adv. Astronaut. Sci.* 158 (October) (2016) 3759–3769.
- [15] O. Çelik, J.P. Sanchez, Opportunities for ballistic soft landing in binary asteroids, *J. Guid. Contr. Dynam.* 40 (6) (2017), <http://dx.doi.org/10.2514/1.G002181>.
- [16] J.P. Sánchez, D. Garcia Yarnoz, C. McInnes, Near-Earth asteroid resource accessibility and future capture mission opportunities, *Global Space Exploration Conference, International Astronautical Federation, Washington, USA, 2012 May 22–24, Paper number: GLEX-2012.11.1.5x12412*.
- [17] V. Szebehely, *Theory of Orbits*, Academic Press, New York, 1967.
- [18] S. Tardivel, D.J. Scheeres, P. Michel, S. van Wal, P. Sanchez, Contact motion on surface of asteroid, *J. Spacecraft Rockets* 51 (6) (2014) 1857–1871, <http://dx.doi.org/10.2514/1.A32939>.
- [19] S. Ulamec, C. Fantinatti, M. Maibaum, K. Geurts, J. Biele, S. Jansen, L. O'Rourke, Rosetta lander-landing and operations on comet 67P/Churyumov-Gerasimenko, *Acta Astronaut.* 125 (August–September) (2016) 80–91, <http://dx.doi.org/10.1016/j.actaastro.2015.11.029>.
- [20] H. Yano, T. Kubota, H. Miyamoto, T. Okada, D. Scheeres, Y. Takagi, K. Yoshida, M. Abe, S. Abe, O. Barnoun-Jha, Touchdown of the Hayabusa spacecraft at the muses sea on Itokawa, *Science* 312 (5778) (2006) 1350–1353, <http://dx.doi.org/10.1126/science.1126164>.
- [21] J. Biele, S. Ulamec, M. Maibaum, R. Roll, L. Witte, E. Jurado, P. Munoz, W. Arnold, H.-U. Auster, C. C., et al., The landing(s) of Philae and inferences about comet surface mechanical properties, *Science* 349 (6247) (2015) 1–6, <http://dx.doi.org/10.1126/science.1259816>.
- [22] J. Biele, L. Kessler, C. D. Grimm, S. Schröder, O. Mierheim, M. Lange, T.-M. Ho, Experimental Determination of the Structural Coefficient of Restitution of a Bouncing Asteroid Lander arXiv:1705.00701. URL <http://arxiv.org/abs/1705.00701>.
- [23] T. Ho, J. Biele, C. Lange, AIM MASCOT-2 Asteroid Lander Concept Design Assessment Study, *Tech. rep. German Aerospace Center (DLR)*, 2016.
- [24] S. Sawai, J. Kawaguchi, D.J. Scheeres, N. Yoshikawa, M. Ogasawara, Development of a target marker for landing on asteroids, *J. Spacecraft Rockets* 51 (4) (2014) 1857–1871, <http://dx.doi.org/10.2514/1.A32304>.
- [25] T. Kubota, S. Sawai, T. Hashimoto, J. Kawaguchi, Collision dynamics of a visual target marker for small-body exploration, *Adv. Robot.* 51 (14) (2014) 1857–1871, <http://dx.doi.org/10.1163/156855307782227426>.
- [26] O. Çelik, J.P. Sanchez, O. Karatekin, B. Ritter, Analysis of natural landing trajectories for passive landers in binary asteroids: a case study for (65803) 1996GT Didymos, 5th Planetary Defence Conference, 2017, <http://dx.doi.org/10.13140/RG.2.2.34443.90405> May 15–19. Paper number: IAA-PDC17-03-P03.
- [27] L. Dell'Elce, N. Baresi, S. Naidu, L. Benner, D. Scheeres, Numerical investigation of the dynamical environment of 65803 Didymos, *Adv. Space Res.* 59 (5) (2016) 1304–1320, <http://dx.doi.org/10.1016/j.asr.2016.12.018>.
- [28] F. Damme, H. Hussmann, J. Oberst, Spacecraft orbit lifetime within two binary near-Earth asteroid systems, *Planet. Space Sci.* 149 (November) (2017) 1–9 <https://dx.doi.org/10.1016/j.pss.2017.07.018>.
- [29] R. Walker, D. Binns, I. Carnelli, M. Kueppers, A. Galvez, CubeSat opportunity payload intersatellite network sensors (COPINS) on the ESA asteroid impact mission (AIM), *Proceedings of the 5th Interplanetary CubeSat Workshop, Oxford, UK, 2016 May 24–25, Paper number 2016. B.1.2*.
- [30] G. Gomez, A. Jorba, J.J. Masdemot, C. Simo, Study of the transfer from the earth to a halo orbit around the equilibrium point L1, *56 (4) (1992) 541–562*.
- [31] O. Çelik, O. Karatekin, B. Ritter, J.P. Sanchez, Reliability analysis of ballistic landing in binary asteroid 65803 (1996GT) Didymos under uncertainty and GNC error considerations, *Proceedings of 26th International Symposium on Spaceflight Dynamics, Vol. ists14, Matsuyama, Japan, 26th, 2017, June 3–9 Paper number: a90510*.
- [32] F. Ferrari, M. Lavagna, Ballistic landing design on binary asteroids: the AIM case study, *Adv. Space Res.* (2017) 1–16, <http://dx.doi.org/10.1016/j.asr.2017.11.033>.
- [33] E. Canalias, A. Blazquez, E. Jurado, T. Martin, Philae descent trajectory computation and landing site selection on comet Churyumov-Gerasimenko, *Proceedings of 23rd International Symposium on Spaceflight Dynamics, Pasadena, California, 2012 Oct 29–Nov 2, Paper number GC-2*.
- [34] J.-P. Sanchez, O. Çelik, Landing in binary asteroids: a global map of feasible descent opportunities for unpowered spacecraft, *International Astronautical Congress (IAC), Adelaide, Australia, 2017 September 25–29, Paper number: IAC-17,C1,8,7,x37745*.
- [35] M. Casasco, J. Gil-Fernandez, G. Ortega, I. Carnelli, Guidance navigation and control challenges for the ESA asteroid impact mission, 30th International Symposium on Space Science and Technology (ISTS 2017), Matsuyama, Japan, 2017, June 3–9, pp. 1–6.
- [36] W.E. Wiesel, *Modern Orbit Determination*, Aphelion Press; Ohio, 2003.
- [37] M. Ceriotti, J.P. Sanchez, Control of asteroid retrieval trajectories to libration point orbits, *Acta Astronaut.* 126 (September–October) (2016) 342–353, <http://dx.doi.org/10.1016/j.actaastro.2016.03.037>.